Prokhorenko V. M., Prokhorenko D. V., Zvorykin C. O., Hainutdinov S. F.

National Technical University of Ukraine «Igor Sikorsky Kyiv Polytechnic Institute». Ukraine, Kyiv

KINETICS OF STRAINS DURING SINGLE-PASS FUSION WELDING OF A SYMMETRICAL BUTT JOINT

The paper presents the results of temperature kinetics and axial strains that are influence on the formation of temporary and residual stress-strain state of the welded joint.

The principal differences in the character of residual longitudinal plastic strains distribution in comparison with the approximate engineering methods are established.

The results of finite element modeling of the coupled problem of thermo-elasto-plasticity in a symmetrical butt joint with dimensions 600 × 240 × 10 mm, made from 08nc steel are represented for the case of submerged-arc welding. [dx.doi.org/10.29010/88.11]

Keywords: symmetrical butt joint; moving heating source by J. Goldak; temperature kinetics and axial elastic and plastic strains.

Introduction

The basic ideas about the stress-strain state (SST) during welding were formed for many years by the leading scientists in this field, including E.O. Paton, G.A. Nikolaev, V.A. Vinokurov, N.O. Okerblom, V.I. Makhnenko, L.M. Lobanov and others.

Basic information concerning SSS is represented in the educational and scientific literature both for students of welding speciality in technical universities of different countries, and for the welding specialists in manufacturing, in design organizations, as well as for researchers at universities, academics and research institutes [1-8].

The field of knowledge about the stress-strain state during welding is difficult enough for studying by students of university, since it represents a separate branch of science about thermo-elasto-plasticity, which is related to a scientific speciality "Mechanics of a deformable solid body".

Students of the welding direction at technical universities usually do not study such disciplines like theory of elasticity, theory of plasticity, continuum mechanics and other related disciplines. Most of the time, education in this direction is limited to courses such as strength of materials or applied mechanics. Therefore, for the students of welding direction such discipline as "Stresses and strains during welding" was included into their curriculum.

In some cases, special sections that are concerning SSS during welding are included in other disciplines of the curriculum (such as "Welded constructions", "Analysis & design of welded structures", "Theory of welding processes", etc.).

Such steps were aimed at developing rather simple and approximate one-dimensional flow patterns of complex phenomena of a metal elasto-plastic deformation in the high-temperature region of a welded joint during welding and subsequent cooling.

However, in most cases these simplified schemes are not accurate enough, which subsequently leads to significant errors in the evaluation and interpretation of the final results of the residual SSS calculations in the structure under study. To justify this approach, reference was made to the methodical side of facilitating the study of this area of knowledge, which is necessary for a future welding technologist for his further work.

At present time, the introduction of computer technology into scientific research has advanced considerably, in particular, the use of powerful specialized engineering and scientific computing systems based on the use of finite element method (FEM).

Owing to computer modeling in many areas of knowledge, including the area of SSS during welding, new more reliable data and ideas about the real phenomena of non-stationary welding heating and cooling of the metal were obtained. At the level adapted for students to understand, this knowledge should be introduced into the practice of the educational process in universities, forming students with a more realistic understanding of the nature of the phenomena under study.

As it is known [1-8], the reason of the residual SSS formation during welding is the residual plastic strains, that formed not only in the weld metal itself, but also in the zones adjacent to the weld.

In general case, for each point of the zone of plastic strains in a complex structure or a simple welded joint

in the chosen system of rectangular coordinates *XYZ*, plastic stains are forming the following tensor

$$\varepsilon_{ij}^{p} = \begin{vmatrix} \varepsilon_{xx}^{p} & \gamma_{xy}^{p} & \gamma_{xz}^{p} \\ \gamma_{yx}^{p} & \varepsilon_{yy}^{p} & \gamma_{yz}^{p} \\ \gamma_{zx}^{p} & \gamma_{zy}^{p} & \varepsilon_{zz}^{p} \end{vmatrix}. \quad (1)$$

For geometrically simple welded joints and structures in the zones of plastic strains in the base metal of a relatively small welded joint or a large-sized welded structure, these strains are well studied both by calculation and experimental methods [6-16].

At the same time, nowadays, at the Welding Production Department of the Igor Sikorsky Kyiv Polytechnic Institute, fundamentally new important results on the kinetics of formation during the process of welding and cooling, as well as the distribution of residual plastic strains in the weld metal were obtained [17-19].

These results could not be obtained when developing the approximate engineering methods for SSS calculating during welding [7-11] within the acceptance of many simplifying assumptions.

Among the assumptions made, first of all, it is necessary to note the following ones: a) uniaxiality of the SSS in the welded joint or welded structure as a result of welding; b) the validity of the flat sections hypothesis for total longitudinal strains during stages of heating, cooling and in the residual state; c) simplified temperature dependence of elastic strains which are correspond to the yield limit of the metal (PRANDTLE diagram); d) independence of thermophysical properties of metal from temperature; e) limitation of plastic strains mechanisms to only one sliding mechanism, which is valid for temperatures of metal that not exceed $0.4 \cdot T_{melt}$; f) simultaneity of the welded seam execution along its entire length (which does not happen in any technological process of welding); g) ignoring (by default), due to unknown, of the actual flowing kinetic processes of elasto-plastic deformation occurring in the weld metal crystallizing from a molten form, from the moment the crystallization of the weld begins and until the welded joint or structure is completely cooled after welding, etc.

It is normal that with such assumptions engineering methods of the SSS calculation during welding provided in overwhelming majority of cases for real welded constructions insufficiently acceptable results. This remark, first of all, refers to the diagram's shape of the residual longitudinal plastic strains in the cross section of the welded joint, which, according to engineering methods, has a form of curvilinear trapezium with a negative sign (residual longitudinal plastic shortening).

In fact, as it follows from the solution of the coupled thermo-elasto-plastic problem by the finite element method (FEM), it is not so simple. The diagram of the residual longitudinal plastic strains for the middle cross-section of the welded joint looks as shown in Fig. 11, which will be discussed in more detail below.

This results from a detailed study of the kinetics of elasto-plastic deformation on the basis of mathematical modeling of the SSS during welding with the use of FEM. In the engineering approximating methods, the maximum plastic shortening on a part of the base metal cross-section area adjacent to the weld on its two sides is unreasonably extended to the cross-section zone of the molten weld metal.

This resulted in further significant errors in the calculation of the residual relative volume of longitudinal plastic strain (in this case — shortening), the value of the conditional longitudinal force (in this case — shrinkage) and, finally, the residual change in the length of the welded joint as a whole (in this case — shortening).

With such approach to the question, as it will be shown below, the errors are of fundamental importance — instead of the residual shortening of the whole joint when accepting the validity of the planar cross-section hypothesis (PCSH), a residual elongation is obtained when accepting the same PCSH, the conditional force is not a shrinkage one (with the sign "–"), but stretching (with the sign "+").

The character of the longitudinal change in the length of the joint is such that the weld with the adjacent zones of the base metal is lengthened, and the side outermost areas of the joint are shortened, moreover, unevenly across the cross-section, and this does not correspond to the PCSH.

Therefore, the use of PCSH for the longitudinal change in length of even such a relatively narrow (240 mm) joint is indeed unacceptable.

Our results of mathematical modeling of the SSS during welding show that in the cross-section of the joint there is a fundamentally different diagram of the residual longitudinal plastic strains. This results in a different distribution of residual longitudinal displacements of the joint. Below, the new obtained and important results will be represented in more details.

Investigation problems

Purpose and objectives of the study

Purpose of the study: Determination of the distribution character of longitudinal plastic strains across the cross-section of the welded joint in whole, and especially, determination of their kinetics and values for the residual state in the model's grid nodes of the highly heated joint zone.

This is of fundamental importance for nodes temporarily passing through the zone of the molten weld metal (for a short time interval ~16 s). Achieving of

this purpose is supposed to be based on detailed tracking and comparison of the kinetics of various strain types in the model's grid nodes of the welded joint that are listed below.

So, in this paper temperature — $\alpha T(t)$, axial plastic — $\varepsilon^p_{xx}(t)$, $\varepsilon^p_{yy}(t)$, $\varepsilon^p_{zz}(t)$, axial elastic — $\varepsilon^e_{xx}(t)$, $\varepsilon^e_{yy}(t)$, $\varepsilon^e_{zz}(t)$, sum of axial plastic and elastic — $\varepsilon_{xx}(t) = \varepsilon^p_{xx}(t) + \varepsilon^e_{xx}(t)$, $\varepsilon_{yy}(t) = \varepsilon^p_{yy}(t) + \varepsilon^e_{yy}(t)$, $\varepsilon_{zz}(t) = \varepsilon^p_{zz}(t) + \varepsilon^e_{zz}(t)$ strains are considered.

Strain kinetics is studied according to the charts plotted on the basis of the FEM calculated data obtained as a result of solving the coupled thermomechanical problem for the grid model of the welded butt joint with dimensions $600 \times 240 \times 10$ mm, made from 08пс steel during its heating along the axial line of the upper surface plane by submerged arc welding at the input heat energy 4000 J/mm. For FEM calculations the heating source model by J. Goldak was used [20].

Research Objectives:

- Development of calculation model of the welded butt joint for implementation of FEM;
- FEM solution of the coupled thermo-elasto-plastic problem for the investigated welded joint;
- Obtaining new calculated data on temperature kinetics, various strains, on the temporary and residual SSS in the welded joint;
- Discussion and analysis of the obtained calculated results and formulation of general conclusions.

Main part

Welded seam in the butt joint with dimensions $600 \times 240 \times 10$ mm is modeled by heating the plate made from 08пс steel per GOST 1050-88 with the ferritic metal structure in the state of supply with the moving submerged welding arc along it's longitudinal direction in a single pass with full penetration.

The plate is oriented horizontally in its position. The upper horizontal plane of the plate will be called the "upper surface of the welded joint", the bottom one — the "bottom surface of the welded joint". In addition "forward edge", "rear edge", "left side edge" and "right side edge" would be distinguished in the plate. The right hand rectangular coordinate system XYZ with the origin in the central node located on the forward edge of the plate's grid model, the X-axis is directed inside the plate and coincides with its longitudinal axis.

The plate has the characteristic symmetrical central plane sections: longitudinal along the X-axis with the coordinate of the plane section $y = 0$ mm, the middle cross-section along the length of the plate with the coordinate of the plane section $x = 300$ mm and the middle plane section across the thickness with the coordinate of the plane section $z = 0$ mm.

The boundary conditions of three fixing nodes, selected on the edges of the joint outside the high-temperature effect zone of the heating source, allow to simulate the technological fixation of the plate during welding. The welded joint is created by heating the plate with full penetration in single pass along the positive direction of the X-axis from the front edge with the coordinate $x = 0$ mm to the rear edge with the coordinate $x = 600$ mm.

The grid model of the joint is formed from four layers of identical thickness (2.5 mm) with the same structure, shape, sizes, number of straight prismatic elements and their locations in the layer. The total number of elements is 23040. The smallest element is a cube element with an edge length $l = 2.5$ mm. There are 8640 of such elements in the grid model and they are filling the highly heated middle zone along the length and through the thickness of the plate at the width of 25 mm and symmetrically in relation to the plane section $y = 0$ mm.

Two types of elements have the form of a straight prism with the height of 2.5 mm and square bases 5×5 mm (9120 elements) and 10×10 mm (2400 elements). The next two types of elements are also in the form of a straight prism with a height of 2.5 mm and a rectangular trapezoidal base. The dimensions of the trapezoidal bases are 2.5 and 5 mm at a height of 2.5 mm (1920 elements), 5 and 10 mm at a height of 2.5 mm (960 elements).

The plate is heated in a single pass on the following mode: the heating source velocity is 5 mm/s, welding current — $I = 730$ A, arc voltage — $U = 34$ V, arc efficiency — $\eta = 0.85$, heat input rate ~ 4000 J/mm. The heating source passes a plate on all its length for 120 s. Such heating mode provides full and almost uniformly penetration for the plate with thickness 10 mm. A flux pad or a flexible vitrified clay pad is required on the bottom side of the plate along the weld seam for proper formation of the weld's back side.

After the heating process, the plate is completely cooled down during 1200 seconds and then released from the fixings, which are technologically necessary during heating. A residual SSS slowly forms in the weld joint at the cooling stage.

Kinetics of plastic strains in the weld metal.

Different elementary weld metal volumes, depending on their coordinates, can reach the melting point of the steel (1300 °C) within time duration 0 ... 5 s. As such volumes, in our case, a small volumes of a cubic form with an edge length 2.5 mm of the plate's grid model in the heated zone with the weld seam can be considered.

Such volume is conveniently to link with the node of the plate's grid model, considering that the grid node is located in the center of the cube. Then, based on the results of the FEM solution, it is possible to plot the kinetic charts of any process parameter development during welding and cooling, including the com-

ponents of the plastic strain tensor for the selected node of the welded joint grid model.

The kinetics of plastic strains in the grid nodes at the joint cross section at x = 300 mm, located in the high-temperature zone at a distance of up to ~ 15 mm on both sides of the weld axis are of the most interest.

Because of cross section symmetry relatively to its middle, only half of this section with a positive direction of the Y-axis will be considered, concentrating on the grid nodes with the size of a square cell of 2.5 mm.

This zone is located on both sides of the weld seam and is limited to 15 mm from its axis. Let's distinguish 7 vertical lines on one side of the weld, starting from the middle of the weld cross section, on which 5 nodes of the grid are evenly spaced in 2.5 mm increments in the thickness of the plate. The total number of such nodes at half of the cross-section is 35.

It is reasonable to consider not all 5 nodes on one vertical line, but only 3: on the upper surface of the plate, on the bottom surface and at the middle plane. The position of 7 vertical lines, with 5 nodes on each, is determined by the coordinates: y = 0; 2.5; 5; 7.5; 10; 12.5; 15 mm. Each grid node has a five-digit numeric designation. The node numbers and coordinates are given in the legend to the strain kinetics charts that are shown below in the blocks of figures 3—9. Each block contains 3 separate figures for three types of longitudinal strains under consideration, respectively.

Three types of longitudinal strains are considered for each node: elastic $\varepsilon^{e}_{xx}(t)$, plastic $\varepsilon^{p}_{xx}(t)$ and sum of elastic and plastic strains $\varepsilon_{xx}(t) = \varepsilon^{p}_{xx}(t) + \varepsilon^{e}_{xx}(t)$.

In the legends to the charts, in the blocks mentioned above, these strains have specific designations adopted in the computation complex. In particular, the sum of elastic and plastic strains is “STRAIN_XX”, plastic strains are “PLASTIC_STRAIN_XX” and elastic strains are “ELASTIC_STRAIN_XX”.

Fig. 1 shows the temperature change in 3 nodes on the vertical line at y = 0 mm in the cross section of the joint at x = 300 mm. Fig. 2 shows the temperature strain in the same three nodes.

Let's proceed to the analysis of the strains kinetics shown in Fig. 3. Here the charts for the three nodes on the vertical line at y = 0 are presented. The main kinetic changes occur in the time interval of the welding and cooling process ~ t = 50...100 s. In the initial period of the welding process ~ t = 0...50 s there is a zero temperature strain (Fig. 2) in all three nodes.

As the heating source approaches the nodes, the temperature strain “Thermal_Strain_NOD” reaches different maximum values for all three nodes, with a further rapid reduction to zero value at the time t = 60...62,5 s.

At the time t = 60 s the heating source reaches the node #69902 with the coordinate x = 300 mm, the temperature in the node achieves 1300 °C, the weld metal goes to the molten state, all strains in the node are zeroed (Fig. 3), the previous loading history (before melting) of the node disappears.

For the other two nodes #69894 and #69890 on this vertical line, all the processes described before for the node #69902 occur 2.5 seconds later, what can be seen from the chart shown in Fig. 3. The process continues till the moment the crystallization of the weld metal begins, which for the considered nodes begins at time ~ t = 75 s, and already at time t = 77,5 s the temperature strain in all three nodes reaches the value ~ $+ 18 \cdot 10^{-3}$. The temperature change in the nodes is shown in Fig. 1.

From Fig. 3 it can be seen that small elastic strains (they are also total here) appear in the node at time t = 50 s (the coordinate of the heating source at this moment x = 250 mm), which can be explained by the heat wave moving ahead of the heating source and slightly heating the plate metal in front of itself.

The heated zone approaches the nodes and a small longitudinal elastic compression occurs in them. There is no plastic strain in the nodes up to the time t = 52,5 s, including.

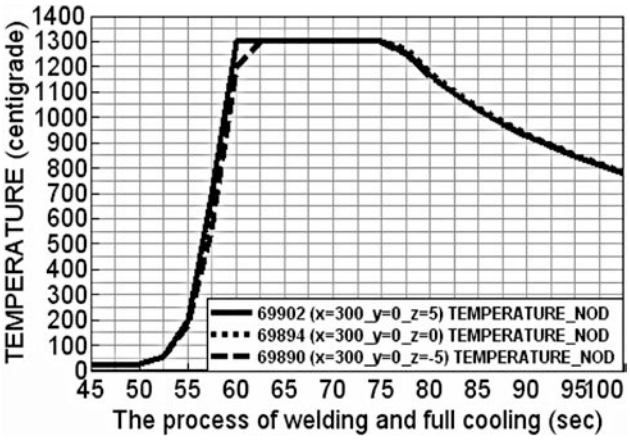

Fig. 1. Temperature in the grid nodes on the weld center line in the cross section at x = 300 mm

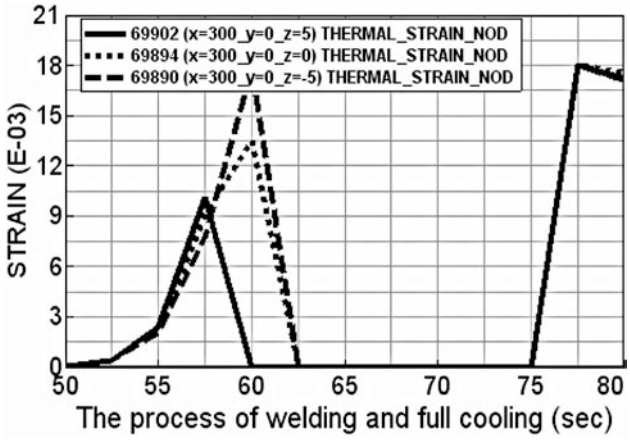

Fig. 2. Temperature strain in the grid nodes at the weld center line in the cross section at x = 300 mm

It appears in the calculation results for the node #69902 only at the time t = 55 s and t = 57,5 s and is of values ~– $0.43 \cdot 10^{-3}$ and ~+ $2.1 \cdot 10^{-3}$, respectively. The second, positive value of this strain is being maximum at the stage of heating the node before the melting of the metal.

From the value of plastic strain ~+ $2.1 \cdot 10^{-3}$ in the node, it is rapidly reduced to zero when the metal melts at the time moment t = 60 s. It is positive and relatively significant because of the large (~– $14.1 \cdot 10^{-3}$) transverse (along the Y-axis) plastic shortening for compensating of which not only the value of plastic elongation along the X-axis equal to ~+ $2.1 \cdot 10^{-3}$ is required, but also the plastic elongation of ~– $12.1 \cdot 10^{-3}$ value along the Z-axis, which actually takes place, and is represented in the calculation results.

For the other two nodes on this vertical line, the analysis can be done in a similar way. The elastic strain of shortening in all three nodes at the time interval t = 40...62,5 s varies within the range from ~– $0.11 \cdot 10^{-3}$ to ~– $1.02 \cdot 10^{-3}$, turning to zero at t = 60...62,5 s.

At the time interval t = 75...77.5 s the temperature strain rapidly increases from zero to the value of ~+ $18 \cdot 10^{-3}$ and synchronously, in this period, the elastic strain in the node #69902 increases from zero to value of ~+ $3.05 \cdot 10^{-3}$, which is equal to ~ 25% of the elastic strain value at the yield limit at normal temperature.

At the same time there is no plastic strain. Total strain is equal to the elastic strain, which can be seen in Fig. 3. Apparently, the properties of the metal at these temperatures are such that the plasticity condition in the analyzed node is not met. At high temperatures, plastic strain develops not by sliding mechanisms, as it takes place at temperatures below $0.4 \cdot T_{melt}$, but mainly by diffusion mechanism.

However, diffusion processes are always slow, while all processes in the #69902 node are flow fast. Plasticity condition in the node #69902, as it can be seen in Fig. 3, begins to be satisfied from the time t = 80 s and from this moment the plastic strain curve of elongation shown on the chart in Fig. 3 (dashed-dotted curve) rapidly increases upwards. In Fig. 3 the difference between the total strain curve (dashed curve) and the plastic strain curve gives the elastic strain curve (pointed curve).

In the second block of charts shown in Fig. 4 the calculation results of the strain kinetics in the nodes located on the vertical line y = 2.5 mm are represented. Kinetics of these strains is similar to that was previously discussed for the nodes on the weld centerline at coordinate y = 0 mm. Since nodes on the vertical line at y = 2.5 mm are located further away from the weld axis, the time metal is being in the liquid phase is 2.5 s less. It should also be noted the peak value of the elastic strain is common to the node located at the middle plane.

On the next vertical line with coordinate y = 5 mm all nodes across the plate thickness fall into the zone of metal melting, charts for them are shown in Fig. 5. For the top node the time interval of metal being in the liquid phase is t = 62.5 ... 72.5 s. For other two nodes downward on the vertical line is t = 65...70 s.

For the middle node across the plate thickness elastic strain at time moment t = 60 s increased to the value ~– $2.55 \cdot 10^{-3}$, which is explained by of the three dimensional stress state formation in the depth of the metal.

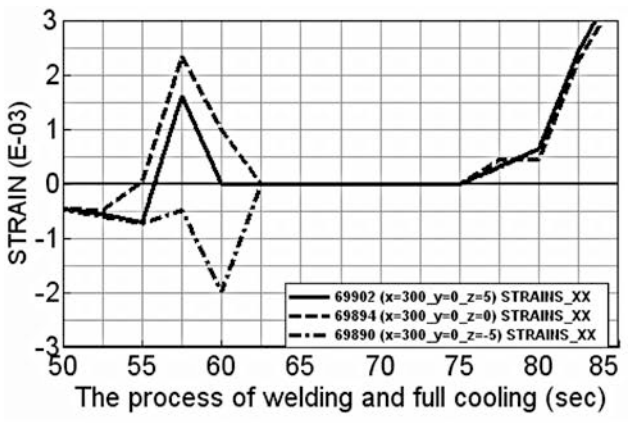

a

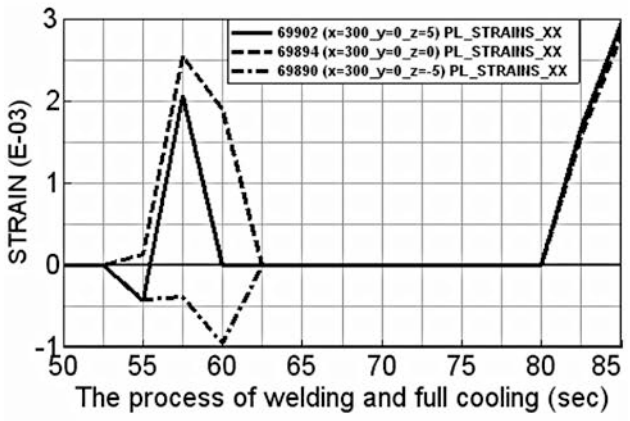

b

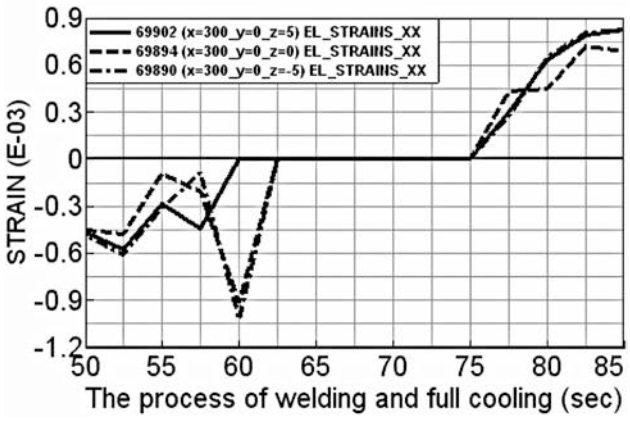

c

Fig.3. Kinetics of longitudinal total (*a*), plastic (*b*) and elastic (*c*) strains in nodes on vertical line at y = 0 mm

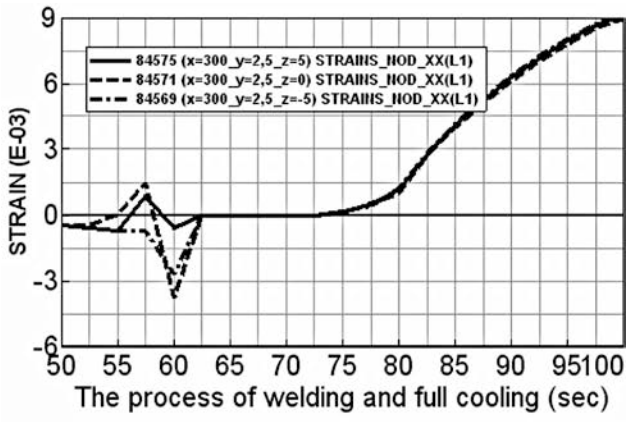

a

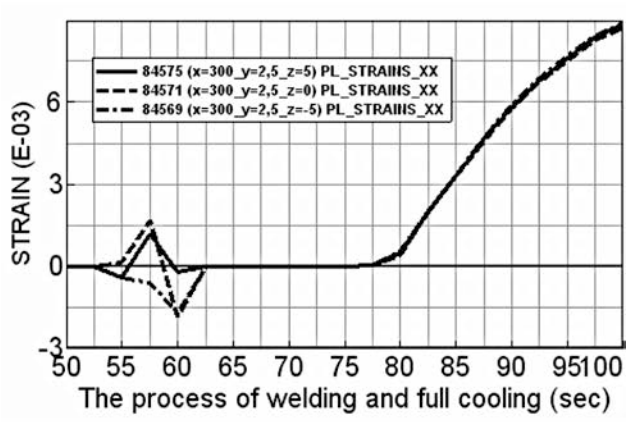

b

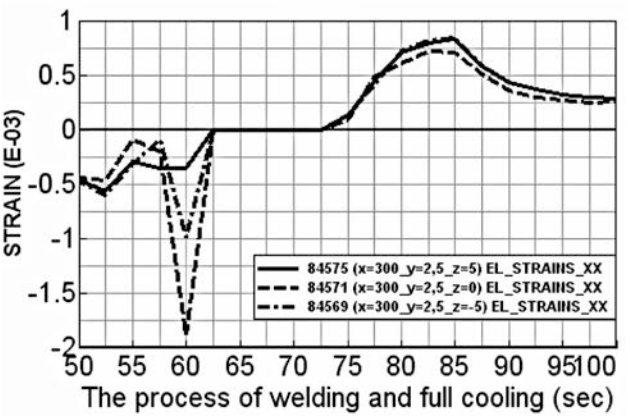

c

Fig. 4. Kinetics of longitudinal total (*a*), plastic (*b*) and elastic (*c*) strains in nodes on vertical line $y = 2.5$ mm

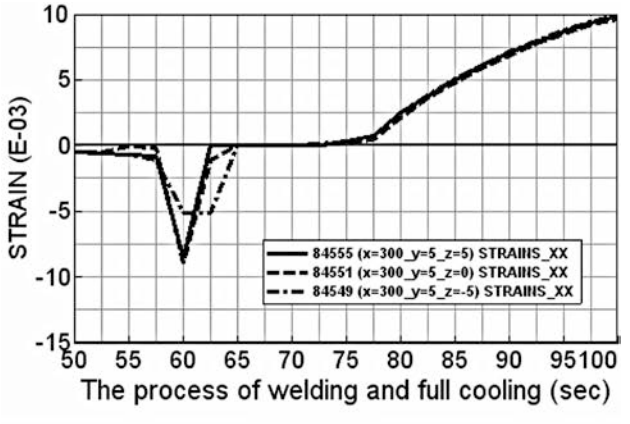

a

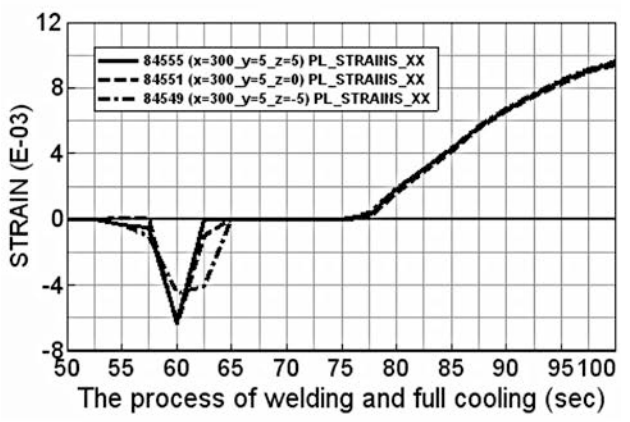

b

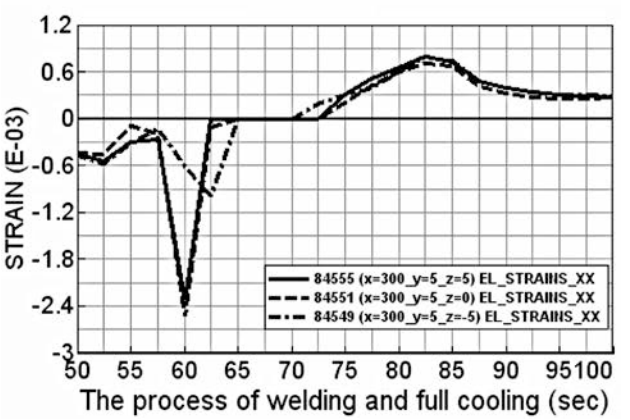

c

Fig. 5. Kinetics of longitudinal total (*a*), plastic (*b*) and elastic (*c*) strains in nodes on vertical line at $y = 5$ mm

At the further away of the vertical line with the considered nodes from the weld axis to the coordinate $y = 7.5$ mm it can be seen (Fig. 6) that only one node #84554 on the upper surface of the plate falls into the zone of molten metal. The molten metal in this node exists in the time interval $t = 67.5...72.5$ s.

From the moment the metal solidification begins in the node #84554 the plastic strain is of a positive sign (stretching). In the lower nodes it continues to be negative for some time, but from the time $t = 75$ s the plastic strain increases and becomes positive in all nodes. For the upper node #84554 the elastic strain of shortening at time $t = 60$ s increases and reaches the value $\sim -3.5 \cdot 10^{-3}$.

At the next step consideration of the nodes #84565, #84561 and #84559 (Fig. 7) on the vertical line with coordinate $y = 10$ mm is required. None of these nodes fall into the zone of molten metal, but at a later stage of cooling for two upper nodes #84565 and #84561 a noticeable plastic elongation can be observed.

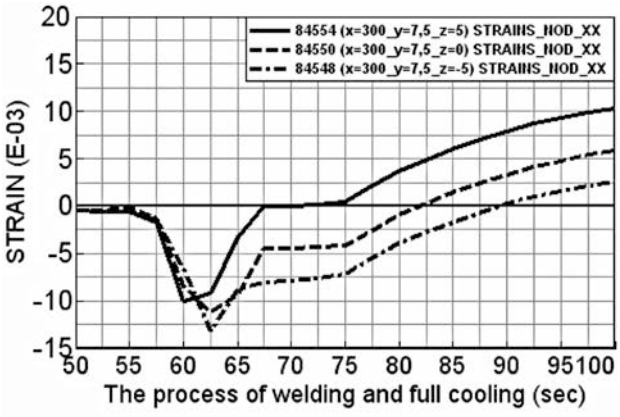

a

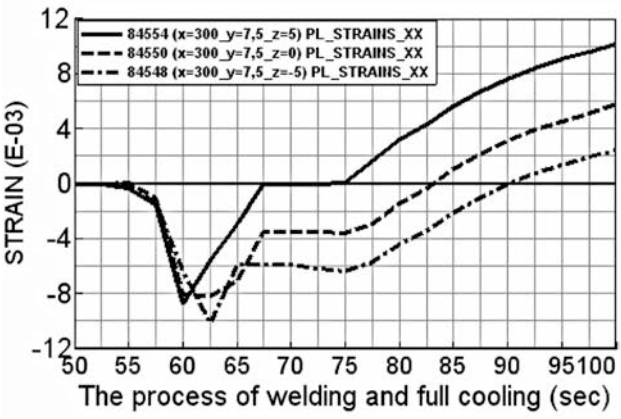

b

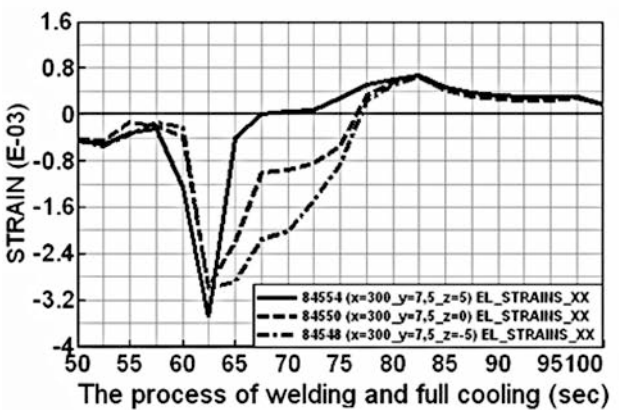

c

Fig. 6. Kinetics of longitudinal total (*a*), plastic (*b*) and elastic (*c*) strains in nodes on vertical line at $y = 7.5$ mm

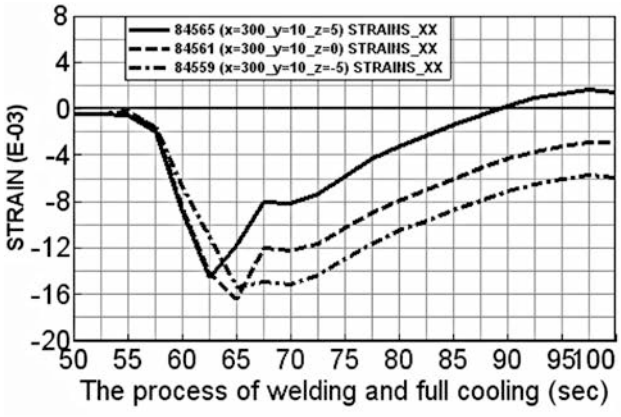

a

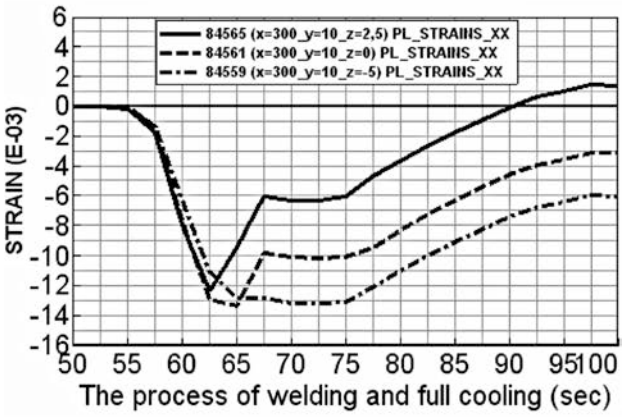

b

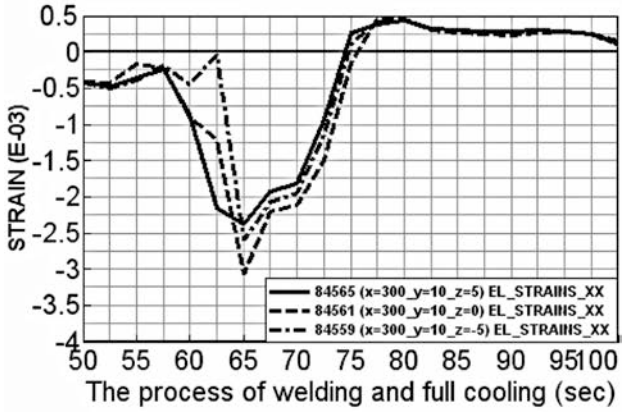

c

Fig. 7. Kinetics of longitudinal total (*a*), plastic (*b*) and elastic (*c*) strains in the zone of non-molten metal near the weld at the vertical line $y = 10$ mm

Plastic shortening of significant value is observed in all nodes on vertical line (Fig. 7) at the time the heating source passing through the middle zone of the welded joint. Intensive heating of this zone leads to the maximum plastic shortening $\sim -13.4 \cdot 10^{-3}$ in the node #84559.

Further cooling of the zone leads to a plastic elongation in all nodes on the vertical line at $y = 10$ mm, which reduces the previous plastic shortening. However, in Fig. 7 it is obvious only for the node #84565 (the curve crosses the abscissa axis). For the node #84561, the plastic strain changes its sign and becomes plastic elongation at a later stage of cooling, which is not visible in Fig. 7.

In the node #84559 the plastic strain in the residual state remains negative (shortening) and equal to $\sim -1.2 \cdot 10^{-3}$. In all nodes on the vertical line at $y = 10$ mm elastic strain up to time $t = 75$ s is also neg-

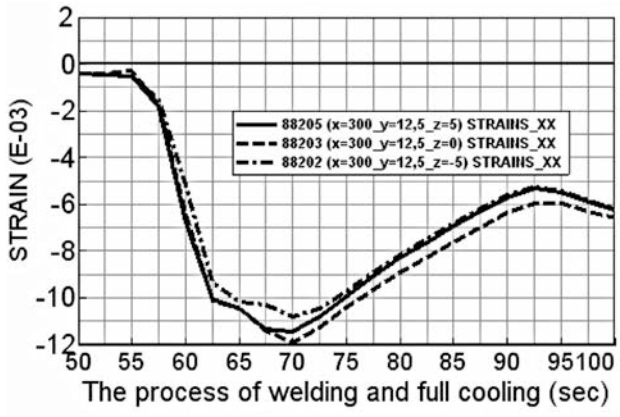

a

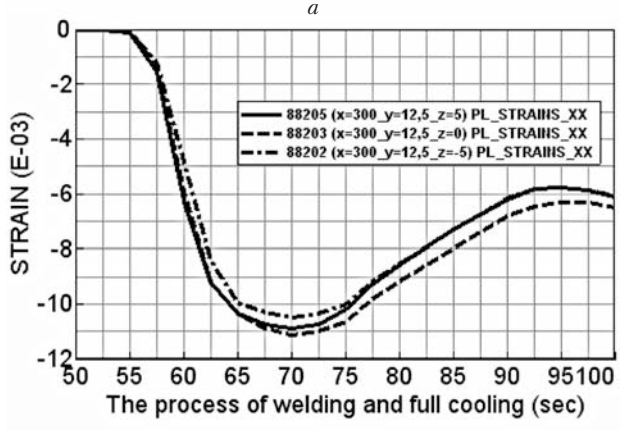

b

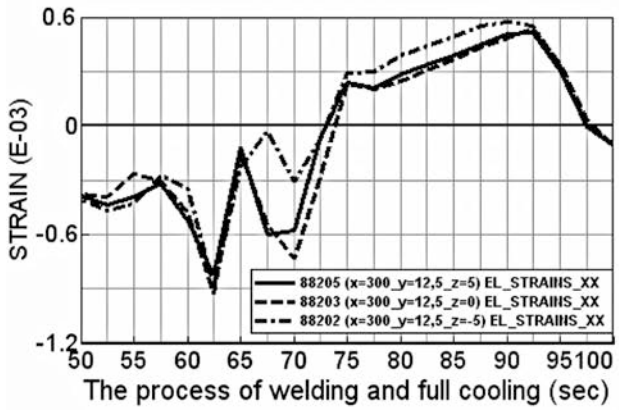

c

Fig. 8. Kinetics of longitudinal total (*a*), plastic (*b*) and elastic (*c*) strains in the zone of non-molten metal near the weld at the vertical line

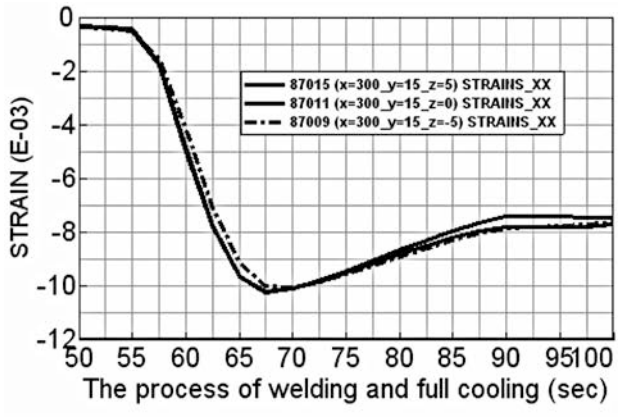

a

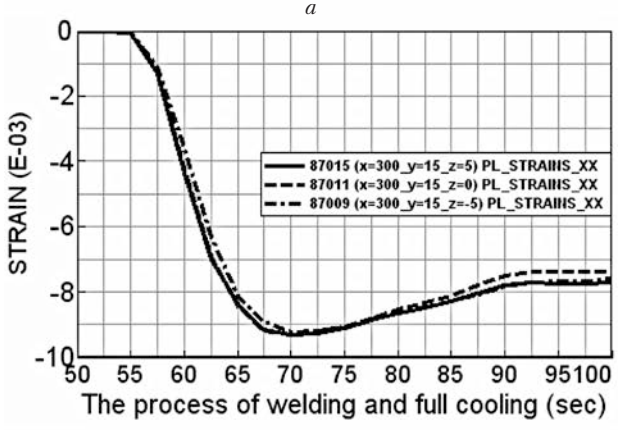

b

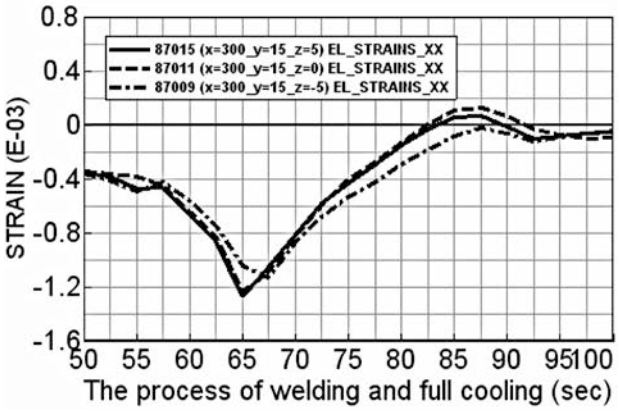

c

Fig. 9. Kinetics of longitudinal total (*a*), plastic (*b*) and elastic (*c*) strains in the zone of non-molten metal near the weld at the vertical line y = 15 mm

ative (shortening), moreover the elastic shortening in the middle node (at the middle plane of the plate) is of significant value $\sim -3.1 \cdot 10^{-3}$, what in ~ 2.6 times exceeds the value that corresponds to the yield limit.

This can only be in the case of a three-dimensional compression stressed state in the node with approximately the equal values of stress components along three coordinate axes. The elastic strain of shortening from the time $t = 75$ s transforms into a slight elastic elongation in all nodes of the considered vertical line at $y = 10$ mm. Fig. 8 shows the results for the vertical line at $y = 12.5$ mm with nodes #88205 (upper surface of the plate), #88203 (middle plane) and #88202 (bottom surface).

The significant values of plastic strains of shortening, shown in Fig. 8, observe at later stages of cooling. They slightly decrease over the time, but remain negative in all nodes to the residual state. For the nodes on

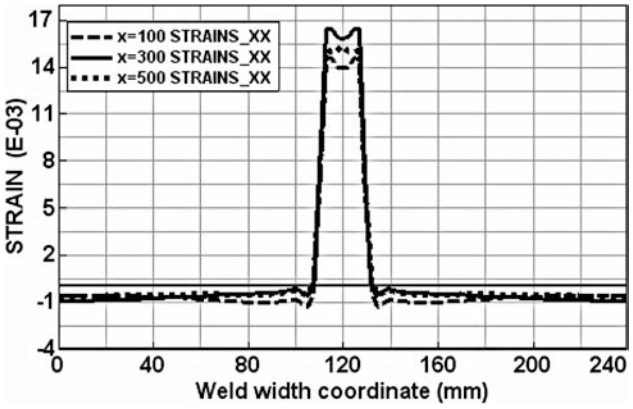

Fig. 10. Total strains along the X-axis in different cross-sections

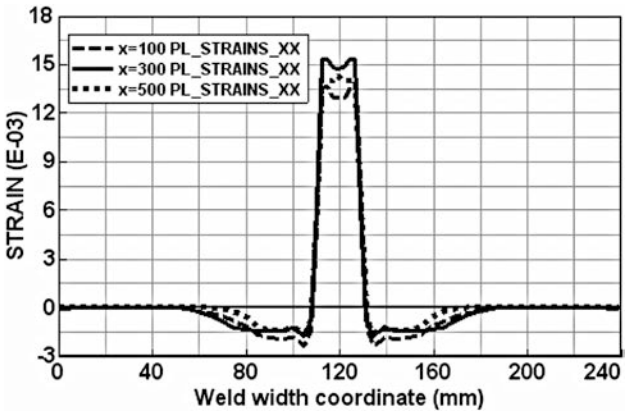

Fig. 11. Plastic strains along the X-axis in different cross-sections

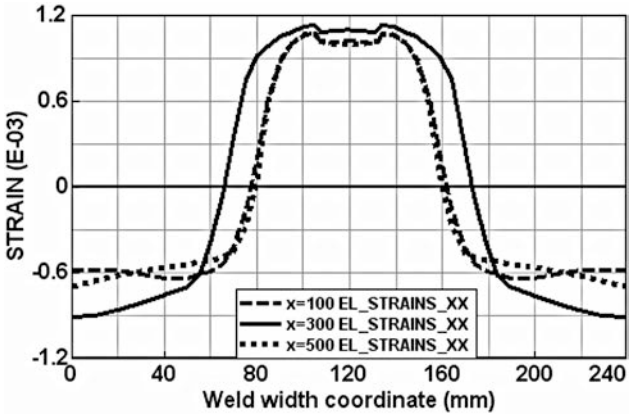

Fig. 12. Elastic strains along the X-axis in different cross-sections

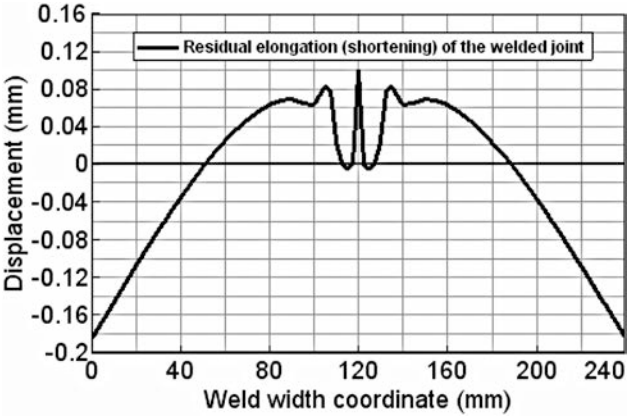

Fig. 13. Distribution of the longitudinal shortening (elongation) in the residual state across the welded joint width

upper and bottom surfaces of the joint the curves coincide and the residual shortening for them is slightly less than for the node #88203 in the middle plane.

For this node, the shortening is much larger (dashed curve), which is apparently associated with a higher three-dimensional stress state in the deep layers across the plate thickness. The elastic strain curves for all nodes cross the abscissa axis at the time t = ~ 115 s and in the residual state (at t = 1200 s) reach values ~$+1.1 \cdot 10^{-3}$ which is close to the yield limit.

The strain kinetics charts for the vertical line at y = 15 mm with nodes #87015, #87011 and # 87009 are shown in Fig. 9. After complete cooling, total and plastic strains have a negative sign (shortening), elastic strain curves for time t = ~ 115 s cross the abscissa axis and take on residual elongation values ~$+1.1 \cdot 10^{-3}$.

In the residual state, the strain curves for all nodes almost coincide. The main conclusion from this block of studies of strain kinetics in the high-temperature zone of the welded butt joint is that in the zone of molten metal from the moment the solidification begins elastic and plastic longitudinal strains of elongation occur simultaneously which continuing to change gradually to the residual state.

For formation of the generalized representation about the residual SSS in the joint the general distributions of residual strains in characteristic cross-sections of the welded joint are of great importance.

In Fig. 10...12 the residual strains "STRAINS_XX", "PL_STRAINS_XX" and "EL_STRAINS_XX" for cross-sections at x = 300, 400 and 500 mm are shown which are total (for the residual state the sum of elastic and plastic strains), plastic and elastic strains respectively.

Fig. 13 shows the distribution of the longitudinal shortening (elongation) in the residual state across the joint width.

Conclusions

1. Melting of the metal in a welding pool, leads to that the entire previous history of its loading disappears. From the moment of solidification at the subsequent cooling the temperature strains appear in the weld metal, as well as elastic and plastic strains along the coordinate axes with realization of all the necessary for this problem equations of elasto-plasticity. The strain values gradually change to the final ones accord-

ing to the conditions of the welding arc heat propagation, fixing in the tooling, external loads and other factors.

2. With the beginning of metal solidification, plastic strains of elongation occur in the weld metal in the direction of the highest stiffness. For the considered butt welded joint, this is the direction along the X-axis (along the weld).

3. According to the principle of non-compressibility of metal at plastic deformation, plastic elongation in the longitudinal direction should be accompanied by plastic shortening at least in one direction, for example, in transverse or in the direction of metal thickness. In our case there is a plastic shortening in two directions — across the width and in direction of metal thickness. This is confirmed by the kinetics charts of the transverse plastic strains and the same strains in direction of metal thickness.

4. The residual longitudinal plastic strains in the melting weld metal in the middle cross-section of the joint have a positive sign (elongation) of a relatively significant value ~+(14.78...15.35) $\cdot 10^{-3}$ depending on the coordinates of the node location in the weld.

5. In the highly heated zone of the base metal adjacent to the weld on both sides, the residual longitudinal plastic strains of shortening within the limits of ~–(1.3...1.6) $\cdot 10^{-3}$ are forming.

6. The residual longitudinal change in the welded joint length is non-uniform across the width, as opposed to how it is determined by approximate engineering methods for a one-dimensional problem, provided that the hypothesis of the planar cross-sections is accepted. Actually, in the residual state the character of the welded joint length changing on its width is defined by a curve shown on Fig. 13.

7. The large value of the residual longitudinal plastic strain of elongation in the weld metal after its previous melting prior to solidification is conditioned by the long interval of temperature strain reduction in the considered node of the joint grid model at the stage of cooling from the moment the solidification begins (1300 °C) and almost to the complete cooling (~128.7 °C). The temperature ~128.7 °C corresponds to the time t = 547.5 s of the welding process and subsequent cooling, which stops further change of the SSS in the joint due to the approaching of the residual state. Temperature change from 1300 °C to 128.7 °C is 1171.3 °C which gives $\alpha \cdot T$ decrease $\Delta\varepsilon_t = \alpha \cdot T = 12 \cdot 10^{-6} \cdot 1171.3 \approx 14.1 \cdot 10^{-3}$ and this with ~10% accuracy overlay the flow rate of $\Delta\varepsilon_t$ for formation of elastic and plastic strain in the node at the cooling stage from the moment the crystallization begins. If for the melting point 1322.46 °C temperature will be accepted instead of 1300 °C, the flow rate $\Delta\varepsilon_t$ for the formation of elastic and plastic strain in the node will be compensated by 100% by reducing the temperature strain during the weld metal cooling from the moment the crystallization begins.

References

[1] Paton, B. E. Tehnologija jelektricheskoj svarki metallov i splavov plavleniem / Pod red. akad B. E. Patona. — M.: Mashinostroenie, 1974. — 768 s. (In Russian)

[2] Vinokurov, V.A. Svarnye konstrukcii. Mehanika razrushenija i kriterii rabotosposobnosti / V.A. Vinokurov, S.A. Kurkin, G.A. Nikolaev. — M.: Mashinostroenie, 1996. — 576 s. (In Russian)

[3] Okerblom, N. O. Konstruktivno-tehnologicheskoe proektirovanie svarnyh konstrukcij / N.O. Okerblom. — L.: Mashinostroenie, 1964. — 420 s. (In Russian)

[4] Mahnenko, V. I. Raschetnye metody issledovanija kinetiki svarochnyh naprjazhenij i deformacij / V.I. Mahnenko. — Kiev: Nauk. dumka, 1976. — 320 s. (In Russian)

[5] Lobanov, L. M. Napruzhennja ta deformacii pri zvarjuvanni i pajanni [Tekst]: pidruchnik /L. M. Lobanov, G. V. Єrmolaev, V. V. Kvasnic'kij, O. V. Mahnenko, G. V. Єgorov, A. V. Labartkava ; za zag. red. L. M. Lobanova. — Mikolaïv: NUK, 2016. — 246 s. — 50 pr. ISBN 978—966—321—310—1. (In Ukrainian)

[6] Prohorenko, V.M. Napruzhennja ta deformacii u zvarnih z'ednannjah i konstrukcijah [Tekst]: navch. posib. / V. M. Prohorenko, O.V. Prohorenko. — K.: NTUU «KPI», 2009. — 268 s. — Bibliogr.: s.267. — 400 pr. ISBN 978-966-622-331-2. (In Ukrainian)

[7] Trochun, I. P. Vnutrennie usilija i deformacii pri svarke / I.P. Trochun. — M. : Mashgiz, 1964. — 248 s. (In Russian)

[8] Vinokurov, V. A. Teorija svarochnyh deformacij i naprjazhenij / V.A. Vinokurov, A.G. Grigor'janc. — M. Mashinostroenie, 1984. — 280 s. (In Russian)

[9] Gatovskij, K.M. Teorija svarochnyh deformacij i naprjazhenij: Ucheb. pos./ K.M. Gatovskij, V.A. Karhin. — Leningr. korablestr. in-t, 1980. — 331 s. (In Russian)

[10] Kuz'minov, S.A. Svarochnye deformacii sudovyh korpusnyh konstrukcij / S.A. Kuz'minov. — L.: Izd. «Sudostroenie», 1974. — 286 s. (In Russian)

[11] Prohorenko, O. V. Rozrobka ta zastosuvannja metodu skladnih pereriziv dlja rozrahunku zalishkovih deformacij vid zvarjuvannja pozdovzhnih shviv odnomirnih konstrukcij [Tekst] : dis. kand. tehn. nauk : 05.03.06 : zahishhena 23.04.07 : zatv. 20.09.07 / Prohorenko Odarka Volodimirivna. — K., 2007. — 249 s. — Bibliogr.: s. 215—224. (In Ukrainian)

[12] Prohorenko, O. V. Rozrahunok zalishkovogo proginu ta tehnologichnih parametriv teplovoï pravki korobchastih balok z dvoma pozdovzhnimi shvami z metoju usunennja proginu [Tekst] / O. V. Prohorenko, V. M. Prohorenko, K. O. Zvorikin // Tehnologicheskie sistemy. — № 2(46). — 2009. — S. 60-66. http://technological-systems.com/index.php/Home/article/view/497/506 (In Ukrainian)

[13] Prohorenko, O. V. Zalishkovij progin hrebtovoï balki vagona vid zvarjuvannja pozdovzhnih shviv [Tekst] // Tehnologicheskie sistemy.— № 4(48). — 2009. — S. 82-93. http://technological-systems.com/index.php/Home/article/view/432/442 (In Ukrainian)

[14] Prohorenko, O. V. Nova koncepcija zapobigannja zalishkovogo proginu hrebtovoï balki vagona vid zvarjuvannja pozdovzhnih shviv [Tekst]/ O. V. Prohorenko, V. M. Prohorenko //Tehnologicheskie sistemy.— № 2(51). — 2010. — S. 58-63. http://technological-zystems.com/index.php/Home/article/view/442/452 (In Ukrainian)

[15] Prohorenko, O. V. Porivnjannja rozrahunkovih shem zvarjuval'nih dzherel tepla za rezul'tatami obchislennja zalishkovogo proginu shtabi pri nagrivi ïï pozdovzhn'oï krajki [Tekst] //Tehnologicheskie sistemy.— № 3(43). — 2008. — S. 67—77. http://technological-systems.com/index.php/Home/article/view/582/592 (In Ukrainian)

[16] Kasatkin, B.S. Eksperimental'nye metody issledovanija deformacij i naprjazhenij / B.S. Kasatkin, A.B. Kudrin, L.M. Lobanov, V.A. Pivtorak, P.I. Poluhin, N.A. Chichenev. — Kiev: Naukova dumka, 1981.- 584 s. (In Russian)

[17] Prohorenko, V.M. Ostatochnoe naprjazhenno-deformirovannoe sostojanie stal'noj polosy pri nagreve prodol'noj kromki dvizhushhimsja istochnikom tepla [Tekst] / V.M. Prohorenko, A.A. Perepichaj, D.V. Prohorenko//Tehnologicheskie sistemy.— № 3(76). — 2016. — S. 112 — 120. — ISSN 2074-0603. / http://technological-systems.com/index.php/Home/article/view/79/87 (In Russian)

[18] Prohorenko, V.M. Ostatochnoe naprjazhenno-deformirovannoe sostojanie stal'noj polosy posle teplovoj pravki progiba prodol'noj osi [Tekst] / V.M. Prohorenko, A.A. Perepichaj, D.V. Prohorenko // Tehnologicheskie sistemy. — №3(80). — 2017. — S. 28-39 — ISSN 2074-0603. [dx.doi.org/10.29010/080.4]/ http://technological-systems.com/index.php/Home/article/view/55/62 (In Russian)

[19] Prokhorenko, V.M. Kinetics of temperature and plastic strains during heating a longitudinal edge of a steel band by moving welding heat source [Text] / V. M. Prokhorenko, D. V. Prokhorenko, S. F. Hainutdinov, A. A. Perepichay //Technological systems. — №3(84). — 2018. — S.63-77. [dx.doi.org/10.29010/084.7] / http://technological-systems.com/index.php/Home/article/view/151/159

[20] Goldak, John A. Computational welding mechanics [Text] / John A. Goldak Mehdi Akhlaghi. — USA: — Springer, 2005. — 325 p.

УДК 621.721.052:539.4.014

Прохоренко В. М., Прохоренко Д. В., Зворыкин К. О., Гайнутдинов С. Ф.

Национальный технический университет Украины «Киевский политехнический институт имени Игоря Сикорского». Украина, г. Киев

КИНЕТИКА ДЕФОРМАЦИЙ ПРИ ОДНОПРОХОДНОЙ СВАРКЕ ПЛАВЛЕНИЕМ СИММЕТРИЧНОГО СТЫКОВОГО СОЕДИНЕНИЯ

В работе представлены результаты кинетики температуры и осевых деформаций, влияющих на формирование временного и остаточного напряжённо-деформированного состояния сварного соединения.

Установлены принципиальные отличия в характере распределения остаточных продольных пластических деформаций в сравнении с приближенными инженерными методами.

Результаты конечно-элементного моделирования связанной задачи термо-упруго-пластичности в симметричном стыковом соединении 600x240x10 мм из стали 08пс представлены для варианта сварки шва плавлением под флюсом. [dx.doi.org/10.29010/88.11]

Ключевые слова: симметричное стыковое соединение; подвижной источник нагрева J. Goldak; кинетика температуры и осевых упругих и пластических деформаций.

Литература

[1] Патон, Б. Е. Технология электрической сварки металлов и сплавов плавлением / Под ред. акад Б. Е. Патона. – М.: Машиностроение, 1974. – 768 с.

[2] Винокуров, В.А. Сварные конструкции. Механика разрушения и критерии работоспособности / В.А. Винокуров, С.А. Куркин, Г.А. Николаев. – М.: Машиностроение, 1996. – 576 с.

[3] Окерблом, Н. О. Конструктивно-технологическое проектирование сварных конструкций / Н.О. Окерблом. – Л.: Машиностроение, 1964. – 420 с.
[4] Махненко, В. И. Расчетные методы исследования кинетики сварочных напряжений и деформаций / В.И. Махненко. – Киев: Наук. думка, 1976. – 320 с.
[5] Лобанов, Л. М. Напруження та деформації при зварюванні і паянні [Текст]: підручник /Л. М. Лобанов, Г. В. Єрмолаєв, В. В. Квасницький, О. В. Махненко, Г. В. Єгоров, А. В. Лабарткава ; за заг. ред. Л. М. Лобанова. – Миколаїв:НУК, 2016. – 246 с. – 50 пр. ISBN 978–966–321–310–1.
[6] Прохоренко, В.М. Напруження та деформації у зварних з'єднаннях і конструкціях [Текст]: навч. посіб. / В. М. Прохоренко, О.В. Прохоренко. – К.: НТУУ «КПІ», 2009. – 268 с. – Бібліогр.: с.267. – 400 пр. ISBN 978-966-622-331-2.
[7] Трочун, И. П. Внутренние усилия и деформации при сварке / И.П. Трочун. – М. : Машгиз, 1964. – 248 с.
[8] Винокуров, В. А. Теория сварочных деформаций и напряжений / В.А. Винокуров, А.Г. Григорьянц. – М. Машиностроение, 1984. – 280 с.
[9] Гатовский, К.М. Теория сварочных деформаций и напряжений: Учеб. пос./ К.М. Гатовский, В.А. Кархин. – Ленингр. кораблестр. ин-т, 1980. – 331 с.
[10] Кузьминов, С.А. Сварочные деформации судовых корпусных конструкций / С.А. Кузьминов. – Л.: Изд. «Судостроение», 1974. – 286 с.
[11] Прохоренко, О. В. Розробка та застосування методу складних перерізів для розрахунку залишкових деформацій від зварювання поздовжніх швів одномірних конструкцій [Текст] : дис. канд. техн. наук : 05.03.06 : захищена 23.04.07 : затв. 20.09.07 / Прохоренко Одарка Володимирівна. – К., 2007. – 249 с. – Библиогр.: с. 215–224.
[12] Прохоренко, О. В. Розрахунок залишкового прогину та технологічних параметрів теплової правки коробчастих балок з двома поздовжніми швами з метою усунення прогину [Текст] / О. В. Прохоренко, В. М. Прохоренко, К. О. Зворикін // Технологические системы. – № 2(46). – 2009. – С. 60-66. http://technological-systems.com/index.php/Home/article/view/497/506
[13] Прохоренко, О. В. Залишковий прогин хребтової балки вагона від зварювання поздовжніх швів [Текст] // Технологические системы.– № 4(48). – 2009. – С. 82-93. http://technological-systems.com/index.php/Home/article/view/432/442
[14] Прохоренко, О. В. Нова концепція запобігання залишкового прогину хребтової балки вагона від зварювання поздовжніх швів [Текст]/ О. В. Прохоренко, В. М. Прохоренко //Технологические системы.– № 2(51). – 2010. – С. 58-63. http://technological-zystems.com/index.php/Home/article/view/442/452
[15] Прохоренко, О. В. Порівняння розрахункових схем зварювальних джерел тепла за результатами обчислення залишкового прогину штаби при нагріві її поздовжньої крайки [Текст] //Технологические системы.– № 3(43). – 2008. – С. 67–77. http://technological-systems.com/index.php/Home/article/view/582/592
[16] Касаткин, Б.С. Экспериментальные методы исследования деформаций и напряжений / Б.С. Касаткин, А.Б. Кудрин, Л.М. Лобанов, В.А. Пивторак, П.И. Полухин, Н.А. Чиченев. – Киев: Наукова думка, 1981.- 584 с.
[17] Прохоренко, В.М. Остаточное напряженно-деформированное состояние стальной полосы при нагреве продольной кромки движущимся источником тепла [Текст] / В.М. Прохоренко, А.А. Перепичай, Д.В. Прохоренко//Технологические системы.– № 3(76). – 2016. – С. 112 – 120. – ISSN 2074-0603. / http://technological-systems.com/index.php/Home/article/view/79/87
[18] Прохоренко, В.М. Остаточное напряженно-деформированное состояние стальной полосы после тепловой правки прогиба продольной оси [Текст] / В.М. Прохоренко, А.А. Перепичай, Д.В. Прохоренко // Технологические системы. – №3(80). – 2017. – С. 28-39 – ISSN 2074-0603. [dx.doi.org/10.29010/080.4]/ http://technological-systems.com/index.php/Home/article/view/55/62
[19] Prokhorenko, V.M. Kinetics of temperature and plastic strains during heating a longitudinal edge of a steel band by moving welding heat source [Text] / V. M. Prokhorenko, D. V. Prokhorenko, S. F. Hainutdinov, A. A. Perepichay //Technological systems. – №3(84). – 2018. – С.63-77. [dx.doi.org/10.29010/084.7] / http://technological-systems.com/index.php/Home/article/view/151/159
[20] Goldak, John A. Computational welding mechanics [Text] / John A. Goldak Mehdi Akhlaghi. – USA: – Springer, 2005. – 325 p.